THE EFFECTS OF BLOOD REHEOLOGICAL ON THE FLOW THROUGH AN AXISYMMETRIC ARTERIAL STENOSIS

Dr. Jafar M. Hassan
Assistant Professor
Department of Mechanical Engineering
University of Technology

ABSTRACT

The prediction of the blood flow through an axisymmetric arterial stenosis is one of the most important aspects to be considered during the Atherosclrosis. Since the blood is specified as a non-Newtonian flow, therefore the effect of fluid types and effect of rheological properties of non-Newtonian fluid on the degree of stenosis have been studied. The motion equations are written in vorticity-stream function formulation and solved numerically. A comparison is made between a Newtonian and non-Newtonian fluid for blood flow at different velocities, viscosity and Reynolds number were solved also. It is found that the properties of blood must be at a certain range to preventing atheroscirasis

الخلاصة

أن عملية تدفق الدم خلال تضيق الشريان المتناظر يعد واحد من أهم الظواهر التي تؤخذ بنظر الاعتبار خلال تصلب الشرايين. وبما ان الدم يصنف من الموائع الغير نيوتينية لذلك تمت دراسة أنواع الموائع وتأثير خواص الدم الغير نيوتيني على درجة تضيق الشريان. كتبت معادلة الجريان بصيغة المسار الدوامي وتم تحليلها عددياً، تمت مقارنة بين المائع النيوتيني و الغير النيوتيني لسرع جريان ولزوجة ومديات رقم رينولد مختلفة . لقد تبين إن خصائص الدم يجب أن تكون ضمن حدود محدودة لغرض منع حدوث حالة تصلب الشريان.

Nomenclature

A_1	Rate of deformation tensor	—
I	Unit tensor	—
J	Jacobian of direct transformation	—
K	Keulegan-Carpenter number	—
n	Power index	—
p	Pressure	N/m^2
Q	Flow rate	m^3/s
R	Radius of the tube at region concerned	m
R_e	Reynolds Number	—
R_{min}	Radius of the tube at the throat	m
R_o	Radius of the tube	m

τ	Period of the imposed flow	s
T	Cauchy `tensor stress	N/ m^2
t	Time	s
t+Δt	Time step	s
u,v	Velocity components in x and r directions	m/s
x,r,t,v,u,p, Λ	Dimensionless variables	—
U_o	Averaged velocity over the section of radius R_o	m/s
	Greek Symbols	
$\eta_o - \eta_\infty$	Asymptotic apparent viscosities	N.s/m^2
$\dot{\gamma}$	Shear rate	1/s
ψ	Stream function	m^3/s
ω	Vorticity	1/s
ρ	Density of the fluid	kg/m^3
Λ	Material parameter	—
λ	Non-dimensional viscosity	—
α	Womersley number	—
ζ, η	Coordinate in the transformed domain	—
α, β, γ	Transformation parameter grid generation	—
δ,σ	Geometrical parameters	m
χ	Dimensional generalized viscosity	N.s/m^2
(x,r,θ)	Cylindrical coordinates system	m
μ	Viscosity of the fluid	N.s/m^2
RF	Relaxation Factor	—
r.h.s	Right Hand Solution	—
S.O.R.	Successive Over Relaxation	—
WBC	Wight Blood Cell	—

INTRODUCTION

The work is concerned with the effect of the Newtonian and non-Newtonian behavior of fluids. Basically, fluid is called non-Newtonian if its viscosity depends on the force that is applied to it. Viscosity is a measure of how easily a fluid flows (the higher the viscosity, the harder it would be to stir a bowl full of it). For example, water has lower viscosity than syrup. For an ordinary fluid (like water) the viscosity wouldn't depend on how fast you were stirring it, but for a non-Newtonian fluid it would. The average velocity in the aorta is about 30 cm/sec that in a capillary is only about 1 mm/sec. It is in the capillaries that exchange of O_2 and Co_2 take place, and this low velocity allows time for diffusion of the gases to occur **[John, 1987].** There is no direct proportionality between shear stress and shear rate for these fluids, there are a large number of rheological equations which describe the flow behavior of these fluids, but there is no single equation which exactly describes the shear stress-shear rate relationship of all these fluids over all ranges of shear rates **[William, 1978]**. The previous is a part of general science of Rheology, rheology as a science is concerned with the study of material that cannot be described by the classical law of Hooke for solids or Newton's law for liquids. That means; it is the science that studies the intermediate material between the above laws.

[Obaid, 1996] stated both Newtonian and non-Newtonian fluid flow cases were investigated for downstream facing step problem .The governing equations solved using a numerical finite element technique. The results are presented for different

Reynolds numbers and for some values of fluids parameter. He found that the length of the separated region grows consistently with Reynolds numbers. Also, the separated region grows slightly with increasing power index (n) when a certain Reynolds numbers have been considered.

[Pontrelil, 2001] presented a differential model of blood flow through a compliant vessel. A nonlinear, viscoelastic, constitutive equation for the wall is coupled with the one-dimensional, averaged fluid momentum equation to describe wave propagation disturbances due to prosthetic implantations, the geometrical, physical and biomechanical parameters need to be carefully identified with reference to a specific flow problem.

The purpose of this work is to study the blood flow over different degree of arterials stenosions, viscosity and Reynolds number.

A computer program using FORTRAN 90 developed to solve the governing equation using finite difference approximation method.

MATHEMATICAL MODEL FOR BLOOD FLOW

While the non-Newtonian approximation for blood flow is acceptable in modeling flow in large arteries and in the propagation of a pressure pulse, a nonlinear constitutive equation has to be used to describe flow in small vessels or at low shear rates, since the average shear rate at the wall of arteries is larger than this value.

Nevertheless, near the center of the vessels, or in separated regions of recirculating flow such as the downstream side of stenosis due to atherosclrosis, the average value of shear rate will be small. Non-Newtonian models take into account the effect of a shear-rate dependent viscosity in some range and reduce Navier-Stokes fluid in some other ranges.

While the plasma is a fluid with no significant departure from Newtonian behavior, when red cells are considered, the viscosity of the whole mixture increases noticeably. Marked Non-Newtonian properties are evidenced for concentrations greater than 10% **[Chien, 1984]**. It is experimentally shown that the blood apparent viscosity decreases as the shear rate increases. In the past years, many constitution equations have been proposed for the blood to model this shear-thinning property **[Mann, 1990]**, **[Phillips, 1975]**,**[Oiknine, 1983]**. Some of them depend on a large number of parameters, while some others are not completely satisfactory in all deformation ranges and for all flows.

Most of such models are based on the following stress – strain rate relationship:

$$T = -\rho I + \mu(\dot{\gamma}) A_1 \qquad (1)$$

Where T is Cauchy‘ s tensor stress. With :

A_1 = grad υ + (grad υ) T

The rate of deformation tensor and its magnitude (i.e. the shear rate):

$$\dot{\gamma} = \left[\frac{1}{2} tr\left(A_1^2\right)\right]^{1/2}$$

In the following expression for the blood viscosity function $\mu(\dot{\gamma})$ is suggested **[Oiknine, 1983]**:

$$\mu(\dot{\gamma}) = \eta_\infty + (\eta_0 - \eta_\infty)\left[\frac{1 + \log_e(1+\Lambda\dot{\gamma})}{1+\Lambda\dot{\gamma}}\right] \qquad (2)$$

Where η_0 and $\eta_\infty (\eta_0 \geq \eta_\infty)$ are the asymptotic apparent viscosities as ($\dot{\gamma} \to 0$ and ∞) respectively, and ($\Lambda \geq 0$) is a material constant with the dimension of time representing the degree of shear-thinning (for $\eta_0 = \eta_\infty$, $\mu(\dot{\gamma}) = constant$ and the model reduces to the Newtonian one) .

The complex nature of blood is approximated here with a three-parameter shear-thinning model, the apparent viscosity μ and the shear rate $\dot{\gamma}$. The apparent viscosity is expressed as a decreasing function of the shear rate $\dot{\gamma}$. Note that, at low shear rates, the apparent viscosity increases considerably. The asymptotic values η_0 are common in many other inelastic shear-thinning models and they are calibrated by best fitting experimental data, while the value of Λ is found by nonlinear regression analysis of viscometric data **[Yeleswarapu, 1996]**.

The Equations of Motion

Blood is assumed to be anisotropic, homogeneous and incompressible continuum, having constant density ρ, and the vessel walls are considered rigid and impermeable. Its viscosity has the expression given by the equation (2).
The equation of motion is :

$$\rho\left(\frac{\partial V}{\partial t} + V \bullet \nabla V\right) = div\, T \qquad (3)$$

where V is the velocity vector and the body forces are supposed negligible.

Let us now consider a cylindrical coordinate system (x, r, θ) having the x – axis coincident with the pipe axis. Because of an axisymmetric two-dimension solution, all variables are assumed independent of θ and the peripheral component of V vanishes.

The pipe has a circular cross section whose radius is R_0 in every where except in a small region centered at (x = 0) with a mild smooth axisymmetric contraction (stenosis), as described by the following function **[Yeleswarapu, 1996]**:

$$R = R_o\left(1 - \mathrm{ST}\left(\frac{1-\cos(\pi x/D)}{2}\right)^2\right),\ 0 \le x \le 2D \qquad (4)$$

Where ST is the degree of the stenosis defined by:

$$\mathrm{ST} = \left(\frac{R_o - R_{\min}}{R_o}\right) 100\%$$

and R_{min} is the radius of the tube at the throat of the constriction.
The vector equation (3) can be written in scalar form:

$$\rho\left(\frac{\partial u}{\partial t} + u\frac{\partial u}{\partial r} + v\frac{\partial u}{\partial x}\right) = -\frac{\partial p}{\partial r} + \mu(\dot{\gamma})\left[\frac{\partial^2 u}{\partial r^2} + \frac{1}{r}\frac{\partial^2 u}{\partial x^2} - \frac{u}{r^2}\right] + 2\frac{\partial \mu}{\partial t}\frac{\partial u}{\partial t} + \frac{\partial \mu}{\partial x}\left(\frac{\partial u}{\partial x} + \frac{\partial v}{\partial r}\right) \qquad (5)$$

$$\rho\left(\frac{\partial v}{\partial t} + u\frac{\partial v}{\partial r} + v\frac{\partial v}{\partial x}\right) = -\frac{\partial p}{\partial x} + \mu(\dot{\gamma})\left[\frac{\partial^2 v}{\partial r^2} + \frac{1}{r}\frac{\partial v}{\partial r} - \frac{\partial^2 v}{\partial x^2}\right] + \frac{\partial \mu}{\partial r}\left(\frac{\partial u}{\partial x} + \frac{\partial v}{\partial r}\right) + 2\frac{\partial \mu}{\partial x} + \frac{\partial v}{\partial x} \qquad (6)$$

Where (u,v) are the components of V in x and r directions respectively.
Let us now introduce a set of nondimensional variables:

$$\mathbf{x} \to \frac{x}{R_0} \qquad \mathbf{r} \to \frac{r}{R_0}$$

$$\mathbf{t} \to \frac{tU_0}{R_0} \qquad \mathbf{u} \to \frac{u}{U_0}$$

$$\mathbf{v} \to \frac{v}{U_0} \qquad \mathbf{p} \to \frac{p}{\rho U_0^2}$$

$$\Lambda \to \frac{\Lambda U_0}{R_0} \qquad \lambda = \frac{\eta_0}{\eta_\infty}$$

With U_0 the velocity averaged over the inlet section of radius R_0.
Moreover, two characteristic nondimensional numbers:

$$\alpha = R_0 \sqrt{\frac{\rho}{\eta_\infty \tau}} \qquad K = \frac{U_0 \tau}{R_0} \tag{7}$$

Are introduced in unsteady flows and are defined as the Womersley and the Keulegan-Carpenter numbers respectively (typically, the characteristic time τ is the period of an imposed flow rate)

In the study case τ is the unit time and equal to R_o/U_o for (K=1), and $\alpha^2 = \frac{\rho R_o U_o}{\eta_\infty}$ is the Reynolds number. The nondimensional counterparts of equations (5)-(6) are cross differentiated and subtracted, to obtain the vorticity – stream function formulation with ω the azimuthal vorticity and ψ the Stokes stream function :

$$\begin{aligned}
&\frac{\partial \omega}{\partial \mathbf{t}} + \left(\frac{1}{\mathbf{r}} \frac{\partial \psi}{\partial \mathbf{r}} \frac{\partial \omega}{\partial \mathbf{x}} - \frac{1}{\mathbf{r}} \frac{\partial \psi}{\partial \mathbf{x}} \frac{\partial \omega}{\partial \mathbf{r}} \right) + \frac{\omega}{\mathbf{r}^2} \frac{\partial \psi}{\partial \mathbf{x}} = \\
&\frac{1}{\alpha^2} \left[\chi \left(\frac{\partial^2 \omega}{\partial \mathbf{x}^2} + \frac{\partial^2 \omega}{\partial \mathbf{r}^2} + \frac{1}{\mathbf{r}} \frac{\partial \omega}{\partial \mathbf{r}} - \frac{\omega}{\mathbf{r}^2} \right) + 2 \frac{\partial \chi}{\partial \mathbf{x}} \frac{\partial \omega}{\partial \mathbf{x}} \right. \\
&+ \frac{\partial \chi}{\partial \mathbf{r}} \left(2 \frac{\partial \omega}{\partial \mathbf{r}} + \frac{\omega}{\mathbf{r}} \right) + 2 \frac{\partial^2 \chi}{\partial \mathbf{r} \partial \mathbf{x}} \left(\frac{1}{\mathbf{r}^2} \frac{\partial \psi}{\partial \mathbf{x}} - \frac{2}{\mathbf{r}} \frac{\partial^2 \psi}{\partial \mathbf{r} \partial \mathbf{x}} \right) \\
&\left. + \left(\frac{\partial^2 \chi}{\partial \mathbf{x}^2} - \frac{\partial^2 \chi}{\partial \mathbf{r}^2} \right) \left(\frac{1}{\mathbf{r}} \frac{\partial^2 \psi}{\partial \mathbf{r}^2} - \frac{1}{\mathbf{r}} \frac{\partial^2 \psi}{\partial \mathbf{x}^2} - \frac{1}{\mathbf{r}^2} \frac{\partial \psi}{\partial \mathbf{r}} \right) \right]
\end{aligned} \tag{8}$$

Where

$$\chi(\dot{\gamma}) = 1 + (\lambda - 1) \frac{1 + \log_e(1 + \Lambda \dot{\gamma})}{1 + \Lambda \dot{\gamma}} \tag{9}$$

$$\begin{aligned}
\dot{\gamma}^2 = &\frac{4}{\mathbf{r}^2} \left[\frac{1}{\mathbf{r}^2} \left(\frac{\partial \psi}{\partial \mathbf{x}} \right)^2 + \left(\frac{\partial^2 \psi}{\partial \mathbf{r} \partial \mathbf{x}} \right)^2 - \frac{1}{\mathbf{r}} \frac{\partial \psi}{\partial \mathbf{x}} \frac{\partial^2 \psi}{\partial \mathbf{r} \partial \mathbf{x}} \right] \\
&+ \frac{1}{\mathbf{r}^2} \left(\frac{\partial^2 \psi}{\partial \mathbf{r}^2} - \frac{1}{\mathbf{r}} \frac{\partial \psi}{\partial \mathbf{r}} - \frac{\partial^2 \psi}{\partial \mathbf{x}^2} \right)^2
\end{aligned} \tag{10}$$

Are the dimensionless generalized viscosity and the squared shear rate, respectively.

The following relation between velocity components, vorticity and stream function holds:

$$\omega = \frac{\partial \mathbf{u}}{\partial \mathbf{x}} - \frac{\partial \mathbf{v}}{\partial \mathbf{r}}$$

$$\mathbf{u} = -\frac{1}{\mathbf{r}}\frac{\partial \psi}{\partial x}$$
$$\mathbf{v} = \frac{1}{\mathbf{r}}\frac{\partial \psi}{\partial \mathbf{r}} \qquad (11)$$

And the equations above to be solved for $0 \le \mathbf{r} \ge 1$.

It is worth noting that the r.h.s. of Eqn. (8) is made up of many terms of different physical significance due to the variable viscosity and express a transport and diffusion of vorticity from the boundary to the main stream. The combined nonlinear effect of these components enters in the dynamics of the vorticity and is important for understanding the formation, the development and the separation of boundary layer. Note that in a fluid with constant viscosity, all the terms in square brackets except the first one disappear.

Vorticity and stream function are related by the Poisson equation:

$$-\omega\mathbf{r} = \frac{\partial^2 \psi}{\partial \mathbf{x}^2} + \frac{\partial^2 \psi}{\partial \mathbf{r}^2} - \frac{1}{\mathbf{r}}\frac{\partial \psi}{\partial \mathbf{r}} \qquad (12)$$

The velocity field, automatically satisfying the continuity equation, can be computed from the stream function. The boundary conditions are required for all boundaries of computational domain since the governing equations are elliptic in partial coordinates. In general, along the boundary of the lower symmetric plane, the stream function is respectively set equal to zero and to a constant value, which is equivalent to one half of the mean mass flow rate through the pipe. The vorticity is zero along the symmetry. On the wall pipe the value of the stream function is uniform, corresponding to an impermeable wall. The value of vorticity on the pipe wall is unknown and must be solved as a part of solution. The inlet boundary condition is uniform flow (u=uniform velocity , v=0) and the outlet boundary of stream and vorticity which is located three periods down stream is imposed to be the same in the stream wise direction. The initial boundary conditions for all variables are zero Fig. (1).

NUMERICAL METHOD

The essence of computational fluid mechanics is the representation of the governing equation in algebraic form suitable for solution by available mathematical techniques. Adopting the finite difference approach, the governing equations that are expressed in the form of differential equations can be represented as finite differences and converted to algebraic equations.

In this part, the vorticity-transport equation ω, stream function equation ψ and the shear rate equation are discretized using the finite difference method with "Time Marching" because it attempts to follow the time evaluation of the flow, in arriving to the steady-state solution.

The approximations for the time derivative in the vorticity equation (8), the numerator is a forward difference for vorticity change occurring at (m,n), from time (t) to (**t** + Δ**t**).

$$\frac{\partial \omega}{\partial \mathbf{t}} = \frac{\omega_{(m,n)}^{i+1} - \omega_{(m,n)}^{i}}{\Delta \mathbf{t}} \qquad (13)$$

Where the ($\omega_{(m+n)}^{i+1}$) is the vorticity at time (**t** + Δ**t**) and the ($\omega_{(m,n)}^{i}$) is the vorticity at (**t**).

The central finite difference approximations are used for convection terms in the vorticity equations as follows:

$$\frac{1}{\mathbf{r}}\left(\frac{\partial\psi}{\partial\mathbf{r}}\frac{\partial\omega}{\partial\mathbf{x}}\right)-\frac{1}{\mathbf{r}}\left(\frac{\partial\psi}{\partial\mathbf{x}}\frac{\partial\omega}{\partial\mathbf{r}}\right)=$$
$$\frac{1}{\mathbf{r}_{(m,n)}}\left[\frac{\psi_{(m,n+1)}-\psi_{(m,n-1)}}{2\Delta\eta}\ \frac{\omega^{i}_{(m+1,n)}-\omega^{i}_{(m-1,n)}}{2\Delta\zeta}\right.$$
$$\left.-\frac{\psi_{(m+1,n)}-\psi_{(m-1,n)}}{2\Delta\zeta}\ \frac{\omega^{i}_{(m,n+1)}-\omega^{i}_{(m,n-1)}}{2\Delta\eta}\right]\Big/J(m,n) \tag{14}$$

$$\frac{\omega}{\mathbf{r}^2}\ \frac{\partial\psi}{\partial\mathbf{x}}=\frac{\omega^{i}_{(m,n)}}{\mathbf{r}(m,n)^2}\left[\frac{\psi_{(m+1,n)}-\psi_{(m-1,n)}}{2\Delta\zeta}\ \mathbf{r}_{\eta}(m,n)\right.$$
$$\left.-\ \frac{\psi_{(m,n+1)}-\psi_{(m,n-1)}}{2\Delta\eta}\ \mathbf{r}_{\zeta}(m,n)\right]\Big/J(m,n) \tag{15}$$

$$\left(\alpha\,\omega_{\zeta\zeta}-2\beta\,\omega_{\zeta\eta}+\gamma\,\omega_{\eta\eta}\right)\Big/J^2=$$
$$\alpha_{(m,n)}\left(\frac{\omega^{i}_{(m+1,n)}-2\,\omega^{i}_{(m,n)}+\omega^{i}_{(m-1,n)}}{2\Delta\zeta^2}\right)$$
$$-2\,\beta_{(m,n)}\left(\frac{\omega^{i}_{(m+1,n+1)}-\omega^{i}_{(m+1,n-1)}-\omega^{i}_{(m-1,n+1)}+\omega^{i}_{(m-1,n-1)}}{4\Delta\zeta\,\Delta\eta}\right)$$
$$+\gamma_{(m,n)}\left(\frac{\omega^{i}_{(m,n+1)}-2\,\omega^{i}_{(m,n)}+\omega^{i}_{(m,n-1)}}{\Delta\eta^2}\right)\Big/J^2_{(m,n)} \tag{16}$$

$$\frac{1}{\mathbf{r}}\left(\omega_{\eta}\,\mathbf{x}_{\zeta}-\omega_{\zeta}\,\mathbf{x}_{\eta}\right)\Big/\,J-\frac{\omega}{\mathbf{r}^2}=$$
$$\frac{1}{\mathbf{r}(m,n)}\left[\frac{\omega^{i}_{(m,n+1)}-\omega^{i}_{(m,n-1)}}{2\Delta\eta}\ \mathbf{x}_{Z}(m,n)\right.$$
$$\left.-\frac{\omega^{i}_{(m+1,n)}-\omega^{i}_{(m-1,n)}}{2\Delta\zeta}\ \mathbf{x}_{e}(m,n)\right]\Big/J_{(m,n)}-\frac{\omega^{i}_{(m,n)}}{\mathbf{r}^2_{(m,n)}} \tag{17}$$

$$2\left(\chi_{\zeta}\,\mathbf{r}_{\eta}-\chi_{\eta}\,\mathbf{r}_{\zeta}\right)\left(\omega_{\zeta}\,\mathbf{r}_{\eta}-\omega_{\eta}\,\mathbf{r}_{\zeta}\right)\Big/J^2=$$
$$2\left(\frac{\chi_{(m+1,n)}-\chi_{(m-1,n)}}{2\Delta\zeta}\mathbf{r}_{e}(m,n)\right.$$

$$-\frac{\chi_{(m,n+1)}-\chi_{(m,n-1)}}{2\Delta\eta}\mathbf{r}_Z(m,n)\Bigg)$$
$$\left(\frac{\omega^j_{(m+1,n)}-\omega^j_{(m-1,n)}}{2\Delta\zeta}\mathbf{r}_e(m,n)-\frac{\omega^j_{(m,n+1)}-\omega^j_{(m,n-1)}}{2\Delta\zeta}\mathbf{r}_Z(m,n)\right)\Big/J^2_{(m,n)} \tag{18}$$

$$\left(\chi_\eta\,\mathbf{x}_\zeta-\chi_\zeta\,\mathbf{x}_\eta\right)/J\left(2\left(\omega_\eta\,\mathbf{x}_\zeta-\omega_\zeta\,\mathbf{x}_\eta\right)/J\right)+\frac{\omega}{\mathbf{r}}=$$
$$\left(\frac{\chi_{(m,n+1)}-\chi_{(m,n-1)}}{2\Delta\eta}\mathbf{x}_Z(m,n)\right.\qquad\left.-\frac{\chi_{(m+1,n)}-\chi_{(m-1,n)}}{2\Delta\zeta}\mathbf{x}_e(m,n)\right)\Big/J(m,n)*\left[2\left(\frac{\omega^j_{(m,n+1)}-\omega^j_{(m,n-1)}}{2\Delta\eta}\mathbf{x}_Z(m,n)\right.\right.$$
$$\left.\left.-\frac{\omega^i_{(m+1,n)}-\omega^i_{(m-1,n)}}{2\Delta\zeta}\mathbf{x}_e\right)\Big/J(m,n)\right]+\frac{\omega^i_{(m,n)}}{\mathbf{r}_{(m,n)}} \tag{19}$$

$$2\left(\chi_{\zeta\eta}\left(\mathbf{r}_\eta\,\mathbf{x}_\zeta-\mathbf{r}_\zeta\,\mathbf{x}_\eta\right)-\chi_{\zeta\zeta}\left(\mathbf{r}_\eta\,\mathbf{x}_\eta\right)-\chi_{\eta\eta}\left(\mathbf{r}_\zeta\,\mathbf{x}_\zeta\right)\right)/J^2=$$
$$2\left(\frac{\chi_{(m+1,n-1)}-\chi_{(m+1,n-1)}-\chi_{(m-1,n-1)}+\chi_{(m-1,n-1)}}{4\Delta\zeta\eta}(\mathbf{r}_e(m,n)\mathbf{x}_Z(m,n)-\mathbf{r}_Z(m,n)\mathbf{x}_e(m,n))\right.$$
$$-\frac{\chi_{(m+1,n)}-2\,\chi_{(m,n)}+\chi_{(m-1,n)}}{\Delta\zeta^2}\left(\mathbf{r}_e(m,n)\;\mathbf{x}_e(m,n)\right)$$
$$\left.-\frac{\chi_{(m,n+1)}-2\,\chi_{(m,n)}+\chi_{(m,n-1)}}{\Delta\eta^2}\left(\mathbf{r}_Z(m,n)\;\mathbf{x}_Z(m,n)\right)\right)\Big/J^2_{(m,n)} \tag{20}$$

$$\frac{1}{\mathbf{r}^2}\left(\psi_\zeta\,\mathbf{r}_\eta-\psi_\eta\,\mathbf{r}_\zeta\right)/J=$$
$$\frac{1}{\mathbf{r}^2_{(m,n)}}\left[\frac{\psi_{(m+1,n)}-\psi_{(m-1,n)}}{2\Delta\zeta}\;\mathbf{r}_e(m,n)\right.$$
$$\left.-\frac{\psi_{(m,n+1)}-\psi_{(m,n-1)}}{2\Delta\eta}\;\mathbf{r}_Z(m,n)\right]\Big/J(m,n) \tag{21}$$

$$\frac{2}{\mathbf{r}}\left(\psi_{\zeta\eta}\left(\mathbf{r}_\eta\,\mathbf{x}_\zeta-\mathbf{r}_\zeta\,\mathbf{x}_\eta\right)-\psi_{\zeta\zeta}\left(\mathbf{r}_\eta\,\mathbf{x}_\eta\right)-\psi_{\eta\eta}\left(\mathbf{r}_\zeta\,\mathbf{x}_\zeta\right)\right)\Big/J^2=$$
$$\frac{2}{\mathbf{r}_{(m,n)}}\left(\frac{\psi_{(m+1,n+1)}-\psi_{(m+1,n-1)}-\psi_{(m-1,n+1)}+\psi_{(m-1,n-1)}}{4\Delta\zeta\Delta\eta}(\mathbf{r}_e(m,n)\mathbf{x}_Z(m,n)-\mathbf{r}_Z(m,n)\;\mathbf{x}_e(m,n))\right.-\frac{\psi_{(m+1,n)}-2\psi_{(m,n)}+\psi_{(m-1,n)}}{\Delta\zeta^2}\;\mathbf{r}_e(m,n)\,\mathbf{x}_e(m,n)$$
$$\left.-\frac{\psi_{(m,n+1)}-2\psi_{(m,n)}+\psi_{(m,n-1)}}{\Delta\eta^2}\;\mathbf{r}_Z(m,n)\,\mathbf{x}_Z(m,n)\right)\Big/J^2_{(m,n)} \tag{22}$$

$$\left(\alpha_x\,\chi_{\zeta\zeta}-2\beta_x\,\chi_{\zeta\eta}+\gamma_x\,\chi_{\eta\eta}\right)/J^2=$$
$$\left(\alpha_x(m,n)\,\frac{\chi_{(m+1,n)}-2\,\chi_{(m,n)}+\chi_{(m-1,n)}}{\Delta\zeta^2}\right.$$
$$\left.-2\,\beta_x(m,n)*\frac{\chi_{(m+1,n+1)}-\chi_{(m+1,n-1)}-\chi_{(m-1,n+1)}+\chi_{(m-1,n-1)}}{4\Delta\zeta\,\Delta\eta}\right.$$

$$+\gamma_x(m,n)*\frac{\chi_{(m,n+1)}-2\chi_{(m,n)}+\chi_{(m,n-1)}}{\Delta\eta^2}\Bigg)\Bigg/ J^2_{(m,n)} \qquad (23)$$

$$\frac{1}{\mathbf{r}}\left(\alpha_R\psi_{\zeta\zeta}-2\beta_R\psi_{\zeta\eta}+\gamma_R\psi_{\eta\eta}\right)/J^2$$
$$-\frac{1}{\mathbf{r}^2}\left(\psi_\eta\mathbf{x}_\zeta-\psi_\zeta\mathbf{x}_\eta\right)/J=$$
$$\frac{1}{\mathbf{r}_{(m,n)}}\Bigg(\alpha_R(m,n)\frac{\psi_{(m+1,n)}-2\psi_{(m,n)}+\psi_{(m-1,n)}}{\Delta\zeta^2}$$
$$-2\beta_R(m,n)\frac{\psi_{(m+1,n+1)}-\psi_{(m+1,n-1)}-\psi_{(m-1,n+1)}+\psi_{(m-1,n-1)}}{4\Delta\zeta\,\Delta\eta}$$
$$+\gamma_R(m,n)\frac{\psi_{(m,n+1)}-2\psi_{(m,n)}+\psi_{(m,n-1)}}{\Delta\eta^2}\Bigg)\Bigg/J^2_{(m,n)}$$
$$-\frac{1}{\mathbf{r}^2_{(m,n)}}\left(\frac{\psi_{(m,n+1)}-\psi_{(m,n-1)}}{2\Delta\eta}\mathbf{x}_Z(m,n)-\frac{\psi_{(m+1,n)}-\psi_{(m-1,n)}}{2\Delta\zeta}\mathbf{x}_e(m,n)\right)\Bigg/J(m,n) \qquad (24)$$

Where α , β and γ are transformation coefficients

$$\alpha = \mathbf{x}_\eta^2 + \mathbf{r}_\eta^2$$
$$\beta = \mathbf{x}_\zeta\,\mathbf{x}_\eta + \mathbf{r}_\zeta\,\mathbf{r}_\eta \qquad (25)$$
$$\gamma = \mathbf{x}_\zeta^2 + \mathbf{r}_\zeta^2$$

And J denotes the Jacobain of the transformation

$$J = \frac{\partial(\mathbf{x},\mathbf{r})}{\partial(\zeta,\eta)} = \mathbf{x}_\zeta\,\mathbf{r}_\eta - \mathbf{x}_\eta\,\mathbf{r}_\zeta \qquad (26)$$

The constant ζ $(\zeta=\zeta(\mathbf{x},\mathbf{r}))$ lines and constant η $(\eta=\eta(\mathbf{x},\mathbf{r}))$ lines can be spaced as desired around the boundaries in the physical domain, since the assignment of the (ζ,η) values to (**x,r**) boundary points via (xi) and (ri) functions are arbitrary, if the shapes of the boundaries shown in Fig. (1) are described.

A computer program developed to solve the above equations. The flow charts shown in figs. (2 and 3).

Results and Discussion

The primary advantages of grids generated by the solution of partial differential equations are smoothness and better control of grid orthogonally at boundary, but the disadvantages are increased computational cost and complexity. So four-grid generation has been generated for four stenosis. Figure (4) shows the grid generation for (0.0), (0.2), (0.5) and (0.8) degree of stenosis.

The parameters that the problem depends on range around some typical values to obtain results of biomechanical interest. They are chosen equal to Newtonian and non-Newtonian fluids to allow a comparison of the two cases. The following physical parameters are assigned in equation (7): K=1 and α^2=10. Therefore,

Reynolds number Re =K * α^2 = 10 is within the physiological range of blood flow in small vessels and rheological parameters (λ, Λ) are (40, 50) **[Chien, 1984]**.

The differences between Newtonian and non-Newtonian flows become significant as shown in Figure (5), the shear rate of Newtonian flow is greater than that of non-Newtonian flow it is positive at the stenosis which the non-Newtonian because a negative at the stenosis due to the effect of viscosity which related to a vortices at the outlet of the stenosis. The effect of dimensionless viscosity (λ) shown in Figure (6) increasing λ the shear rate increases because the viscosity of blood depends on the Hematocrit. Where, the Hematocrit is a centrifuge or a device for separating the cells and on other particulate elements of the blood from the plasma.

Figure (7) shows the velocity profiles for non-Newtonian fluid of Re=10, 20, 50 and 300 for 0.8 degree of stenosis. Figure (8) shows the shear stress for non-Newtonian fluid at Re (10, 20, 50 and 300) for 0.8 degree of stenosis. The shear increases with decrease in the degree of stenosis. From Figures (7 and 8) it is found that the flow rates, and the different properties which affect the blood flow such as pressure drop, viscosity, length and radius of the vessel, which are the main parameters that cause the atherosclerosis. The heart tries to increase the velocity of blood and this velocity is periodic (pulsating), to try to open the stenosis so the recirculation is greater at 0.8 degree of stenosis. The flows of non-Newtonian fluid of Re=50 and degrees of stenosis equal to 0.2, 0.5, and 0.8 are simulated. The streamline of Re=50 for the three stenosis is shown in Figure (9) the marked effects that the degree of stenosis has on the flow field. Whereas for 0.2 degree of stenosis there is no vortex formed and even for 0.5 degree of stenosis there is a small recirculation zone, for 0.8 degree of stenosis the recirculation zone is dominant in the flow field.

The shear rate for non-Newtonian fluid of Re=50 and degree of stenosis equal to 0.2, 0.5 and 0.8 is shown in Figure (10) the shear rate increases when the degree of stenosis decreases, which leads to adverse pressure gradient.

Figures (11 and 12) shows that increasing the viscosity will lead to decrease the velocity at the wall even for constant diameter which leads to thromboses. The increasing in the viscosity called the polycythaemia. This increase is due to decreases in the total volume of plasima or increase the total volume of the red cells. That cause deficiency of oxygen to the tissue. The symptoms for this case, headache, thromboses, cyanosis and itching. It is treated by blood letting which lead to regenerating the red cell and therefore the viscosity of blood will reduce.

CONCLUSIONS

Mathematical models and numerical simulations offer an alternative and non-invasive tool for obtaining detailed and realistic descriptions of complex arterial flows.

A simulation of the blood flow through a stenotic arterial segment has been carried out. Although the important effect of unsteadiness is disregarded, this work shows the combined role played by the geometry and the material nonlinearity on the flow field.

The results demonstrate that the non-Newtonian character of the blood, in some typical regions, modify the flow pattern, even beyond the contracted region, reduce the shear stress at the wall a cross the tenosis. Therefore the presented model is able to predict the main characteristics of the physical flows and may have some interest in biomedical applications. An estimate of the characteristic parameters should be addressed on the basis of existing measurements.

The flow field and wall shear-stress distributions that each model induce for different Reynold number and degree of stenosis is investigated and results show that there are marked differences between simulating the blood as Newtonian and as non-Newtonian fluid. The rheological parameters in non-Newtonian fluid (blood) have the normal medical cases where increasing or decreasing these parameters, will leads to up normal in medical cases.

ACKNOWLEDGMENT

I would like to express my faithful gratitude to Dr. Taha Al-Ani specialist in Medicine and Dr. Ayad M. Al-Rawi in Al-Kerama Hospital for their co-operation.

REFERENCES

- Chien, S., Usami, S., Skalak, R., blood flow in small tube, in Hand book of physiology, Sec.2. The Cardiovascular System, Vol. 4, M. renkins, C.C. Michel Eds, American Physiology Society. Bethesda, PP. 217-249, (1984).
- John R. Cameron and James G. Skofronick "Medical Physics", Awiley-Interscience Publication, New York, 1987.
- Mann, D.E., Tarbell, J. M., "Flow of non-Newtonian blood analog fluids in grid curved straight artery modeles", Biorheology, Vol. 27, Pp. 7711-733, (1990).
- Obiad T. A. S., "A finite Element Method for Generatized Newtonian Flow", University of Basrah. Eng. & Technology Vol. 15, No. 5, Pp. 30-40, (1996).
- Oiknine C., "Rheology of the human blood", in Adv. Cardiovasc. Phys., Vol. 5, Part 1, PP. 1-25, Karger. Based, (1983).
- Phillips, W. M., Deutsch, S., Toward a constitutive equation for blood, Biorhelogy, Vol. 12, PP. 383-389, (1975).
- Pontrell G., "modeling the fluid-wall interaction in a blood vessel", Instituto Perle Applicazionidelcalcolo- CNR, Roma, Italy, June, (2001).
- William R. Schowalter, "Mechanics of non-Newtonian Fluid", Princeton University, U.S.A., (1978).
- Yeleswarapu, K. K., Evaluation of continuum models for Characterizing the constitutive behavior of blood, Ph. D. thesis, University of Pittsburgh, (1996).

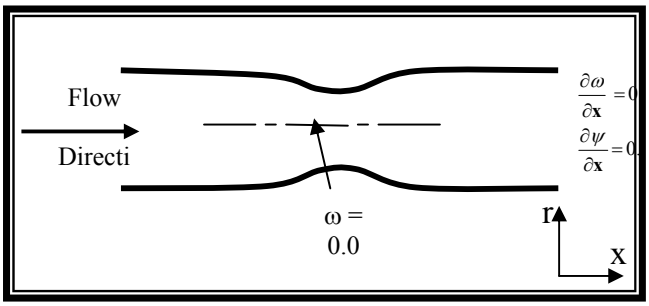

Figure (1) Boundary condition

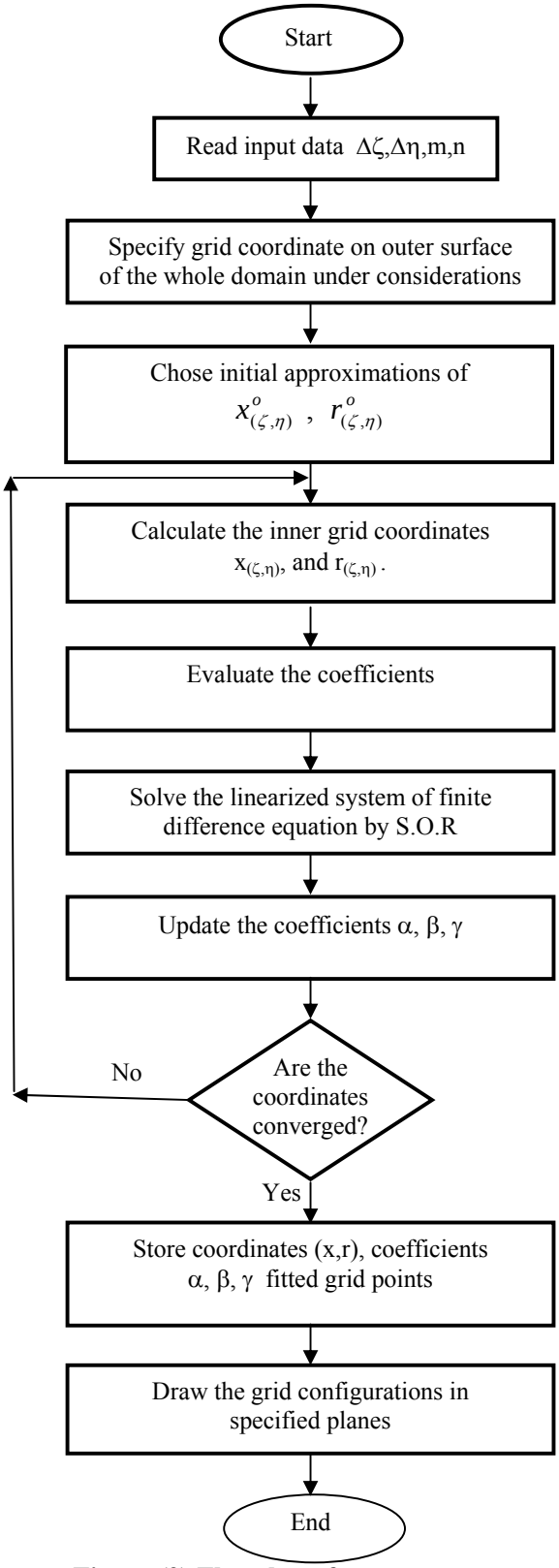

Figure (2) Flowchart for program to create the node grids

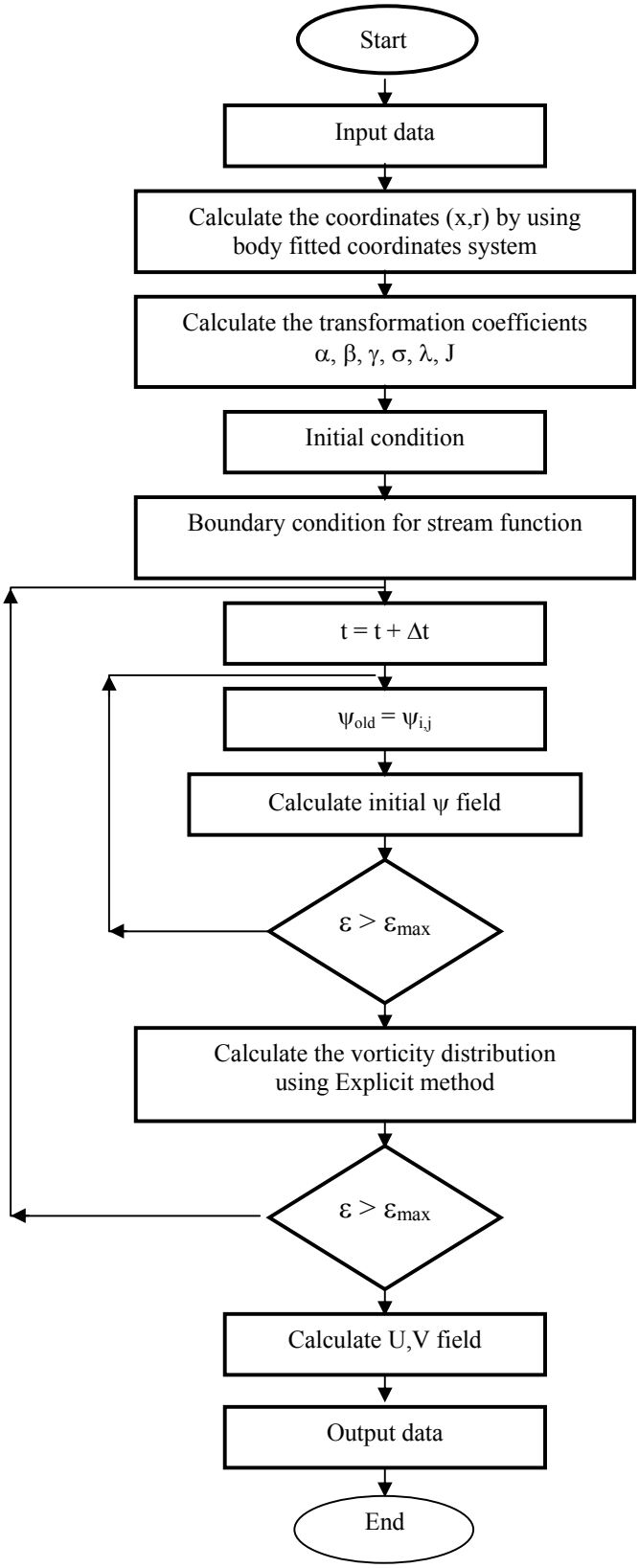

Figure (3) Flowchart for program used to solve the problem

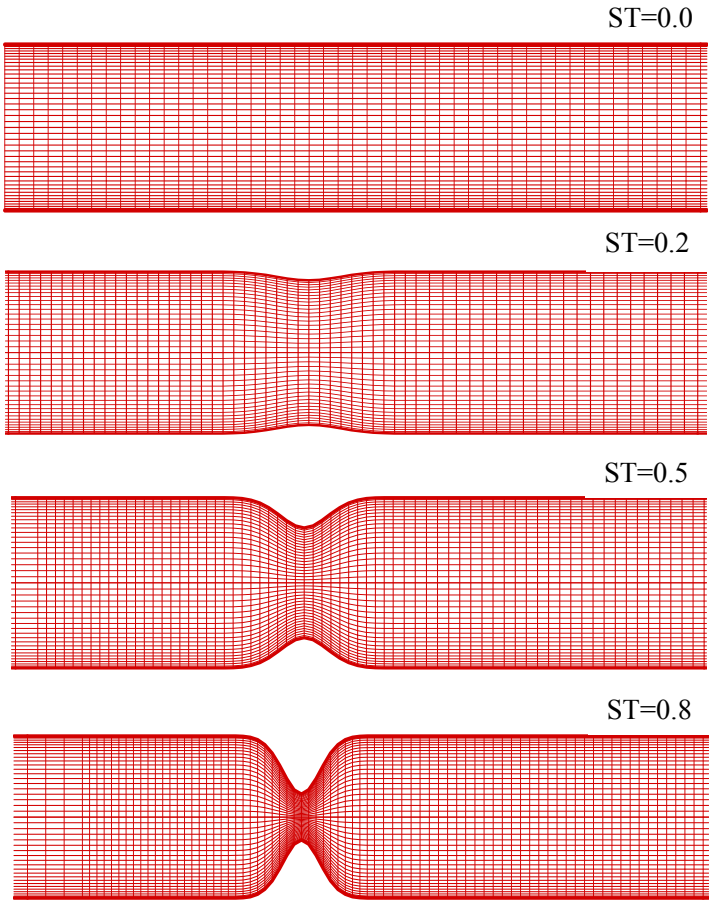

Figure (4) The grid generation for the section of stenosis (0.0),(0.2), (0.5) and (0.8).

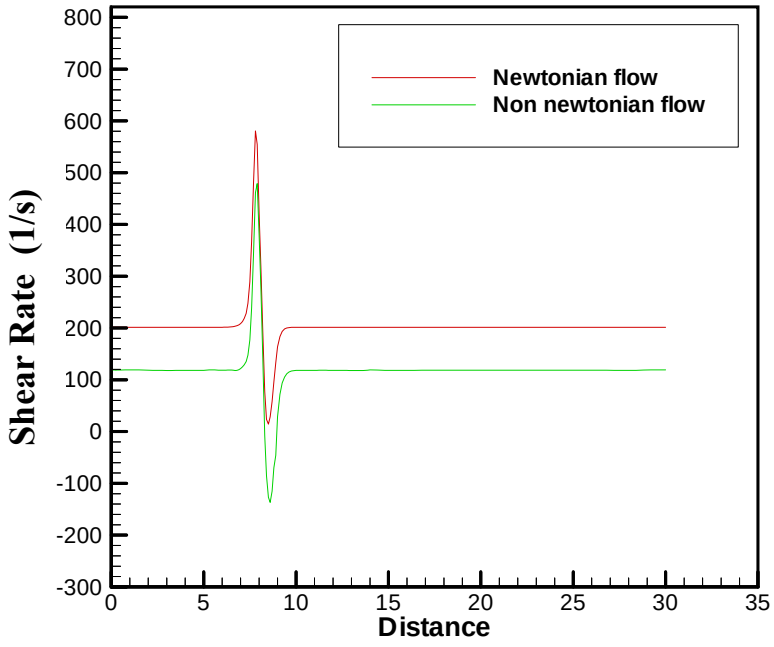

Figure (5) Shear Rate at the wall for Re = 10 (comparison between Newtonian and non- Newtonian)

(x)

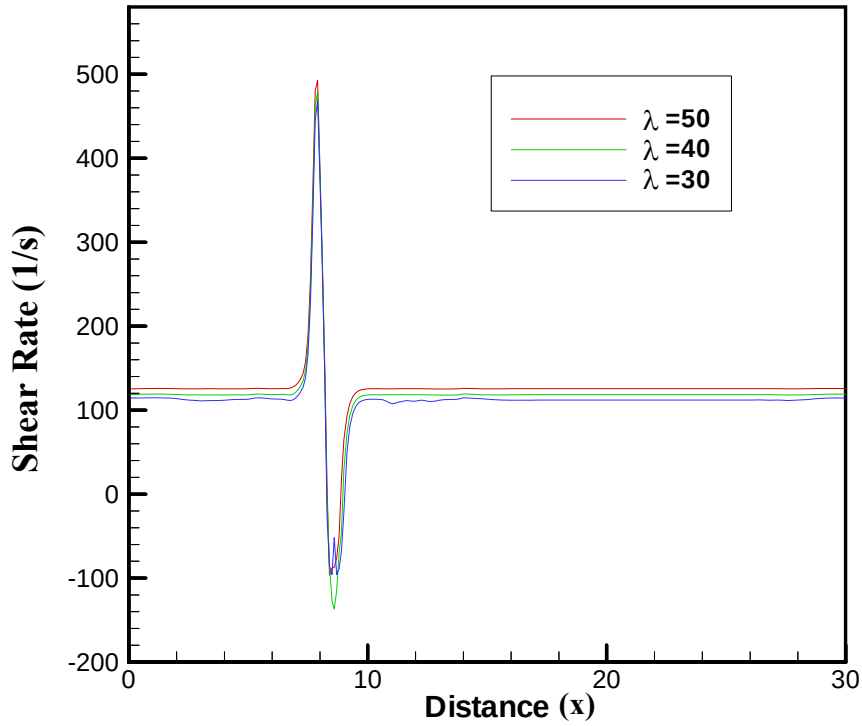

Figure (6) Shear Rate at the wall for Re = 10 and degree of stenosis equal to 0.5 for difference non dimensional viscosities λ= (50, 40, 30).

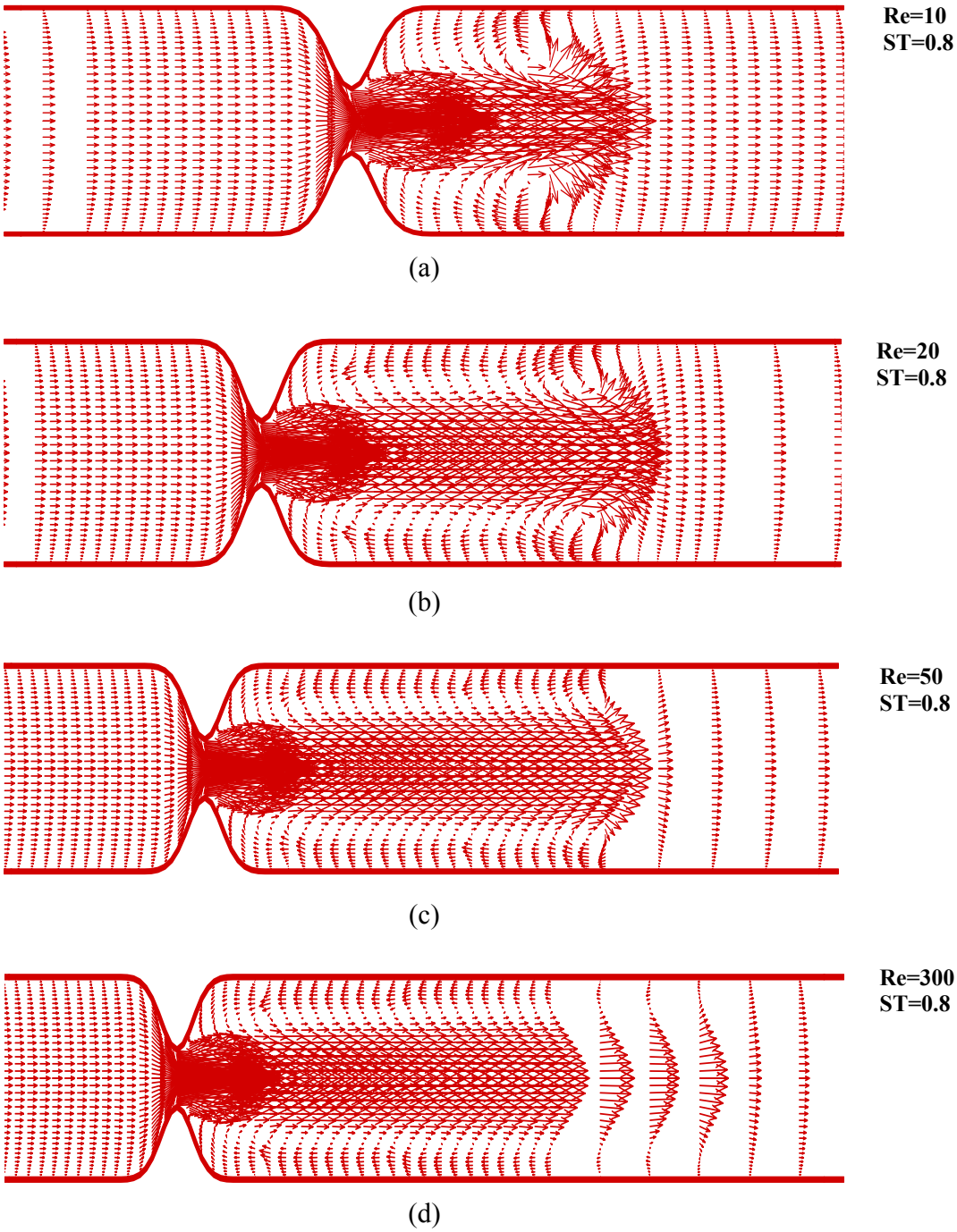

**Figure (7) The velocity profiles for non-Newtonian flow for:
(a) Re = 10 ; (b) Re = 20 ; (c) Re = 50 ; (d) Re = 300
and for 0.8 single degree of stenosis.**

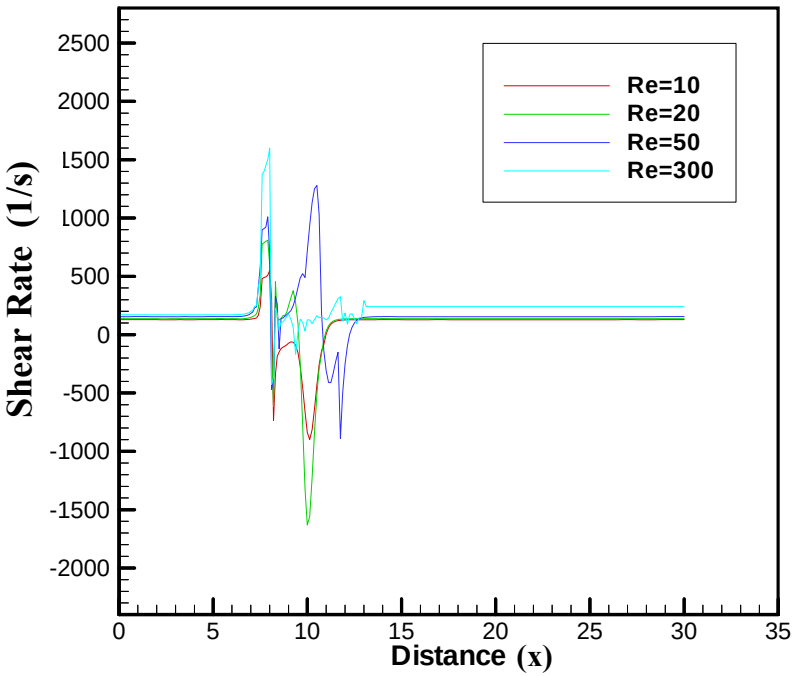

Figure (8) Shear Rate at the wall for Re = 10, 20, 50 and 300 and single degree of stenosis equal to 0.8

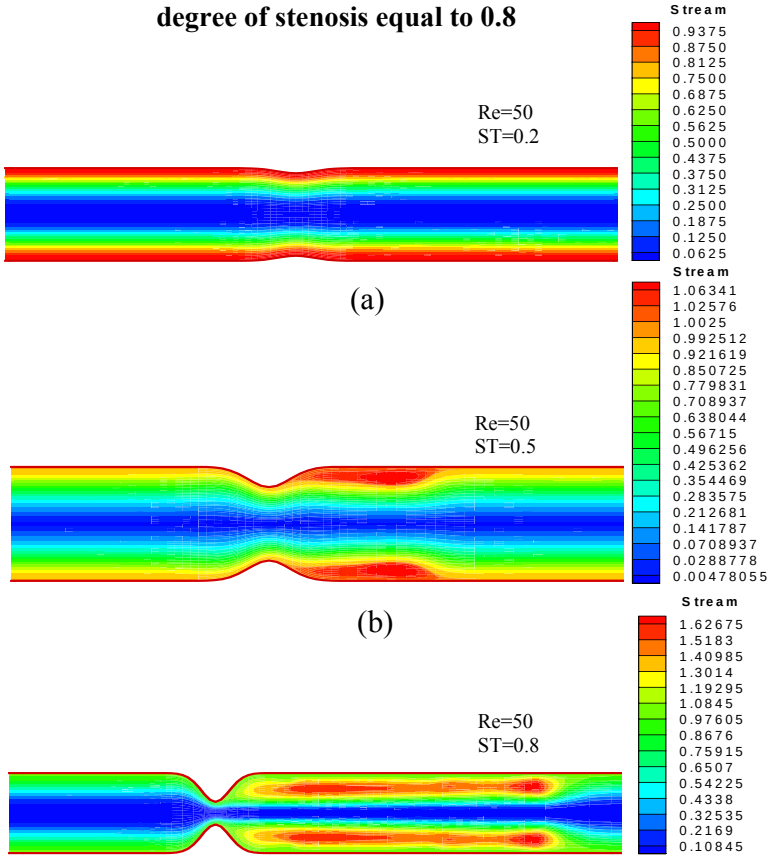

Figure (9) Streamline for non-Newtonian for Re = 50 and for different degrees of Stenosis: (a) 0.2 ; (b) 0.5 ; (c) 0.8.

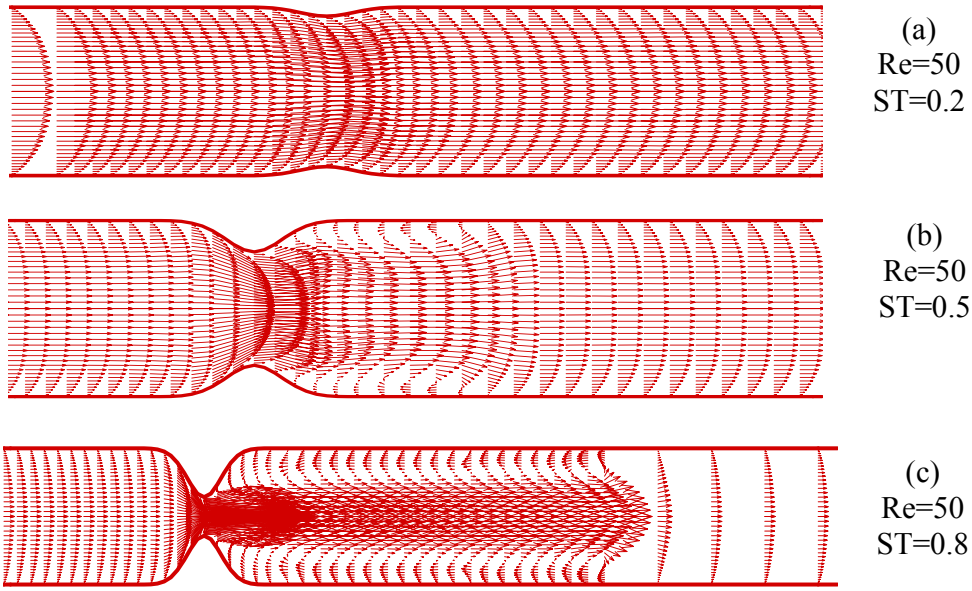

Figure (10) The velocity profile for non-Newtonian flow for Re = 50 and for different degrees of stenosis (a) 0.2 ; (b) 0.5 ; (c) 0.8

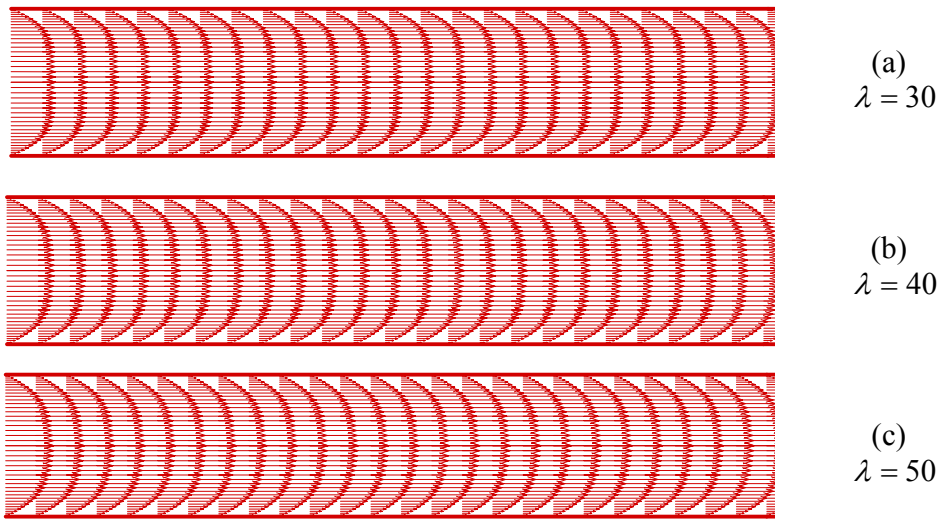

Figure (11) The velocity profile for non-Newtonian flow for Re=300, ST=0.0

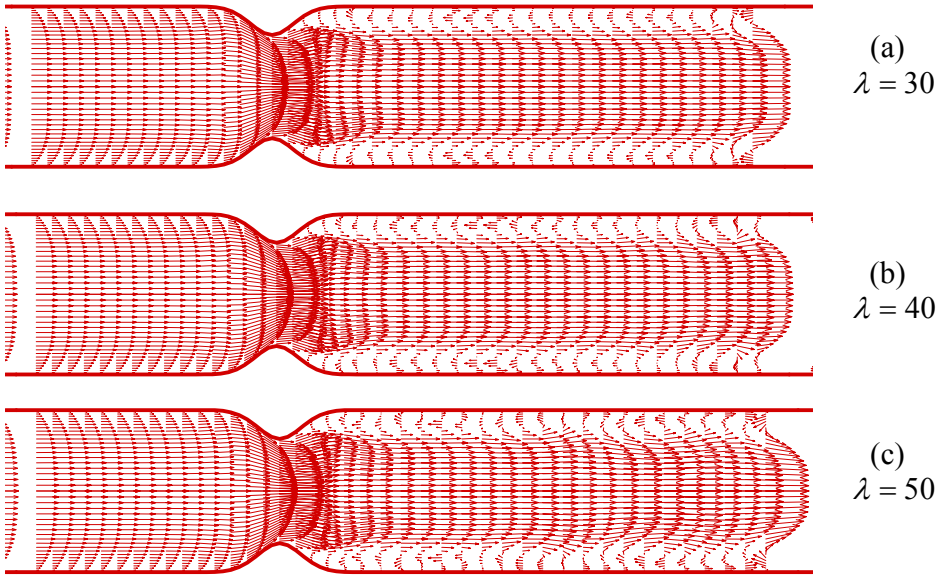

Figure (12) The velocity profile for non-Newtonian flow for Re=300, ST=0.5